ACS OMEGA

Open Access

http://pubs.acs.org/journal/acsodf

Article

Antimicrobial Peptide-Loaded Mesoporous Silica Nanoparticles: A pH-Triggered Controlled Release against Biofilms

Mirena Sakaj,* Vincenzo Lombardi, Isabella Caligiuri, Andrea Castellin, and Pietro Riello

Cite This: *ACS Omega* 2025, 10, 60142−60151

Read Online

ACCESS | Metrics & More | Article Recommendations | Supporting Information

ABSTRACT: The rapid emergence of multidrug-resistant bacteria has intensified interest in antimicrobial peptides (AMPs) as alternative therapeutics due to their potent broad-spectrum activity and low propensity for inducing resistance. However, the clinical translation of AMPs is hindered by their inherent low stability and susceptibility to proteolytic degradation. In this study, we investigated a pH-responsive delivery system using mesoporous silica nanoparticles (MSNs) to encapsulate frog-derived temporin B and scorpion-derived BmKn2—two AMPs that have shown particular promise—aiming to enhance their stability and enable targeted eradication of *Staphylococcus aureus* biofilms. AMPs were efficiently adsorbed onto MSNs via electrostatic interactions, achieving a high loading capacity. The release of peptides was minimal at physiological pH (7.4) but was significantly accelerated under mildly acidic conditions (pH 5.5), typical of biofilm environments. This tunable release behavior enabled controlled delivery and improved protection of the peptides from enzymatic degradation. In vitro studies demonstrated that AMP-loaded MSNs retained antibacterial and antibiofilm activity against *Staphylococcus aureus*, comparable to that of free peptides, while offering stability. The adaptability of this MSN-based platform to other AMPs with similar physicochemical properties highlights its broader potential for combating resistant bacterial infections.

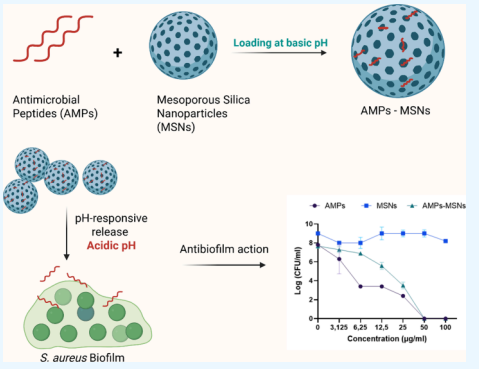

INTRODUCTION

Bacterial infections and biofilm formation are major clinical concerns affecting millions of people worldwide.[1] Chronic infections remain a leading cause of mortality among severely ill, hospitalized patients and pose both a clinical and economic burden to global healthcare systems.[2] The growing incidence of antimicrobial resistance has compromised the efficacy of conventional therapeutics, leading to treatment failures and prolonged hospital stays.[3] A key contributor to this crisis is *Staphylococcus aureus* (*S. aureus*), a Gram-positive pathogen capable of infecting a range of human tissues—from superficial layers such as the skin and eyes to deeper regions such as the heart, bones, and gastrointestinal tract.[4] *S. aureus* is also a common agent of postsurgical infections, especially those involving implanted devices including prosthetic joints and artificial valves, even in developed healthcare settings.[5,6] Eradication of such infections is particularly difficult due to the persistence mechanisms and immune evasion strategy of the bacterium.[7,8] One of the most challenging aspects of *S. aureus* pathogenesis is its ability to form biofilms—complex, structure-adhering bacterial communities embedded within a self-produced extracellular matrix composed of polysaccharides, proteins, and extracellular DNA.[9,10] The biofilm acts as a physical and biochemical barrier, protecting the embedded bacteria from antibiotics and immune cells.[11] Furthermore, the biofilm environment is often more acidic (pH ∼ 5−6.5) than the surrounding healthy tissues.[12,13] The ability of *S. aureus* to adapt to pH variations allows it to colonize diverse niche including the skin, mouth, vaginal tract, abscesses, and even phagolysosomes inside immune cells.[14,15] *S. aureus* infection has long been treated with β-lactam antibiotics.[16] For serious invasive infection caused by MRSA, the current first-line treatment involves glycopeptide antibiotics such as vancomycin and teicoplanin. Despite their potency, these antibiotics present significant limitations due to their intravenous administration route and poor tissue penetration, and their increased resistance further complicates their clinical utility.[17,18] Consequently, the development of alternative therapies capable of overcoming existing resistance mechanisms is essential. To counteract the growing threat of multidrug-resistant pathogens, antimicrobial peptides (AMPs) have emerged as promising alternatives.[19] Typically ranging from 12 to 50 amino acids, they possess an amphipathic structure and are rich in positively charged residues such as lysin and arginine and are grouped into four categories based on the presence of key secondary structures such as α-helices, β-

Received: May 24, 2025
Revised: October 3, 2025
Accepted: October 17, 2025
Published: December 3, 2025

sheets, and various turns and loops.[20,21] This allows them to interact with negatively charged bacterial membranes, causing membrane disruption or interfering with intracellular targets.[22] AMPs exhibit a broad spectrum of antimicrobial, antiviral, antifungal, and even anticancer activity.[23,24] Notably, they demonstrate rapid antibacterial action, low likelihood for resistance development, and potential immunomodulatory functions. In vitro studies have shown that AMPs can be synergistic with traditional antibiotics, enhancing bacterial membrane permeability and antibiotic uptake.[22,25,26] However, despite their promising pharmacodynamics, clinical translation of AMPs is limited. Many AMPs are susceptible to proteolytic degradation in plasma, have poor metabolic stability, and undergo rapid renal clearance, leading to a short systematic half-life.[27,28] To address these limitations, there is a growing interest in developing strategies to enhance the AMP stability and delivery, including peptide engineering and incorporation into nanocarriers.[29] Both organic and inorganic nanoparticles have been explored as delivery systems to improve the AMP pharmacokinetics, control release, and reduce off-target toxicity.[30,31] Among inorganic platforms, mesoporous silica nanoparticles (MSNs) have gained significant attention due to their unique physicochemical properties.[32−34] MSNs offer a high surface area, tunable pore diameter, large loading capacity, and biocompatibility.[33] The release of payloads from MNPs can be triggered by environmental cues such as pH, redox conditions, temperatures, enzymes, or competitive binding agents.[35] Electrostatic interactions are commonly used to load cationic peptides into the negatively charged silica matrix of MSNs.[36] Based on these principles, we investigated the pH-responsive MSN-based platform to deliver two α-helical AMPs—temporin B and BmKn2—two nondisulfide AMPs. Temporin B is a 13-residue peptide derived from the skin of Rana temporary (European red frog), while BmKn2 is a peptide derived from the venom of the scorpion Butkus martensii Karsch.[37,38] Both peptides have shown activity against Gram-positive pathogens including *S. aureus*, with reported minimum inhibitory concentration (MIC) values ranging from 2.5 to 20 μM. In this work, we examined the loading efficiency, pH-dependent release profiles, protease stability, and antimicrobial activity (against planktonic and biofilm forms of *S. aureus*) of AMP-loaded MSNs. Our results demonstrate that both peptides retain their bactericidal and antibiofilm properties after MSN loading and that the peptide release is significantly enhanced under acidic conditions. Moreover, MSNs conferred strong protection against proteolytic degradation. Together, these findings support the potential of MSN-based platforms for delivering AMPs in a controlled and pH-triggered manner, providing a proof of concept for the treatment of biofilm-associated infections and a promising direction for future antimicrobial nanomedicines.

MATERIALS AND METHODS

Materials. Fmoc-protected amino acids, Rink Amide AM resin support, and benzotriazol-1-yloxytripyrrolidinophosphonium hexafluoro phosphate (PyBoP) were purchased from Novabiochem. Trifuoroacetic acid (TFA), triisopropylsilane (TIS), cetyltrimethylammonium bromide (CTABr), tetraethyl orthosilicate (TEOS), ammonia solution (38%), nutrient broth (NB), proteinase K, phosphate-buffer saline (PBS), and agar were purchased from Sigma-Aldrich. The *Staphylococcus aureus* ATCC 25923 strain was obtained from the American Type Culture Collection. The Calgary biofilm device (CBD) was purchased from Innovotech, and MRC-5 cells were purchased from ATCC (Manassas, VA). Cell lines were grown according to the manufacturers' instructions.

Solid-State Peptide Synthesis. Temporin B (LLPIVGNLLKSLL) and BmKn2 (FIGAIARLLSKIF) were synthesized on the MultiPep RSi synthesizer (Intavis) by standard Fmoc solid-phase chemistry on a Rink Amide AM resin (0.01 mmol scale, 100−200 mesh loading 0.52 mmol/g). The coupling step was conducted twice for each amino acid (6 equiv, 0.4 M solution in DMF) using the PyBOP (5.5 equiv, 0.4 M solution in DMF) and NMM (9 equiv, 4 M solution in DMF) coupling system. Fmoc groups were removed using a 20% (v/v) solution of piperidine in DMF. The final peptides were deprotected and cleaved from the resin using a TFA/TIS/water mixture (95/2.5/2.5 v/v) for 3 h at room temperature under vigorous shaking. The peptide was precipitated with cold diethyl ether (50 mL), centrifuged, resuspended, and washed with diethyl ether (20 mL × 2). The peptide was further purified with a preparative reversed-phase high-performance liquid chromatography (RP-HPLC) C18 column, linear gradient with a mobile phase composed of eluent A (99.9% v/v H_2O, 0.1% v/v TFA) and eluent B (99.9% v/v acetonitrile, 0.1% v/v TFA) at a flow rate of 20 mL/min. The purified peptides were freeze-dried and dissolved in Milli-Q water. The purity of the peptides was assessed by analytical RP-HPLC (LC PerkinElmer). The molecular mass was confirmed by liquid chromatography mass spectrometry (LC/MS) analysis (Agilent 1260 Infinity) (Figure S1). Due to the absence of aromatic residues in the peptide sequence, the concentrations were extrapolated from calibration curves generated using six different concentrations in the range of 0.5−0.015 mg/mL using an RP-HPLC C18 column, at a wavelength of 220 nm, and a linear gradient with a mobile phase composed of eluent A (99.9% v/v H_2O, 0.1% v/v TFA) and eluent B (94.9% v/v acetonitrile, 5% v/v H_2O, and 0.1% v/v TFA) at a flow rate of 1 mL/min. The calibration curves show good linearity in the analyzed range of R^2 = 0.999 (Figure S2).

MSN Synthesis. MSNs were synthesized as described elsewhere.[39] In a glass flask, a quantity of CTABr (5.7 g) and ammonia solution (0.38 mL) was dissolved in water (142 mL) and ethanol (48 mL) solution under stirring at room temperature for 15 min at 500 rpm. After the complete solubilization of the compounds, TEOS (5 mL) was added dropwise, and the mixture was stirred vigorously (500 rpm) for 2 h at 30 °C. The final colloidal solution was centrifuged at 9000 rpm, and the recovered solid was washed several times with ETOH and H_2O (50% v/v) and dried at 60 °C overnight. To remove the surfactant, the product was calcined at 550 °C at a rate of 2 °C/min for 5 h. The obtained sample was referred to as MSNs.

AMP Adsorption. Temporin B and BmKn2 (0.5 mg each) were incubated separately with 1 mg of MSNs in PBS at pH values of 5.5, 7.4, and 10 for 24 h, shaking at 150 rpm. Unabsorbed peptides were separated from the MSNs by centrifugation at 12 000 rpm for 10 min and washed twice to remove the remaining unabsorbed peptides. The concentrations of the adsorbed peptides were measured after 24 h of incubation using the RP-HPLC C18 column, following the procedure described above.

AMP Release. The pH-triggered release efficiency of temporin B and BmKn2 from MSNs was assessed at different pH values (5.5, 7.4, and 10). The released peptides were

https://doi.org/10.1021/acsomega.1c04410
ACS Omega 2025, 10, 60142−60151

separated from the MSNs by centrifugation at 12,000 rpm for 10 min, and the peptide concentrations were measured at different time points using RP-HPLC C18, following the procedure described above.

Antibacterial and Antibiofilm Activity. The antimicrobial activity of the peptides was evaluated using a standard liquid dilution method in NB medium. *S. aureus* ATCC25923 cells were cultured overnight at 37 °C in NB, then diluted in the same medium to an initial concentration of 1×10^6 cells/mL. In a 96-well sterile microtiter plate, 50 μL of this bacterial suspension was added to 100 μL of serially diluted peptide solution, resulting in a total volume of 150 μL per well. Concentrations of the peptides loaded onto MSNs range for temporin B from 133 to 1 μg/mL and for BmKn2 from 50 to 1 μg/mL. Empty MSNs (control; 200−2.7 μg/mL) with PBS serve as the final negative control. The 96-well sterile microtiter plates were incubated at 37 °C for 24 h with shaking at 150 rpm. Bacterial growth was assessed by measuring the optical density at 600 nm (OD_{600}) using a Synergy Biotek microplate reader. To account for any interference from the nanoparticles themselves, the optical density of wells containing only the nanoparticles was subtracted from the measured OD values. The MICs were determined as the lowest peptide concentration that completely inhibited bacterial growth (100%).

The antibiofilm activity was assessed using the CBD, employing a 96-well plate with pegs built into the lid, which serve as the surface for biofilm formation. *S. aureus* ATCC25923 was cultured in NB medium and allowed to form biofilm on the pegs for 48 h at 37 °C. Following the biofilm formation, the pegs were rinsed to remove planktonic cells and then transferred to a flat-bottom microtiter plate containing various concentrations of AMPs for an additional 24 h incubation at 37 °C. For both temporin B−MSNs and BmKn2−MSNs, a range of concentrations similar to the MIC determination was used, adjusting as necessary based on the initial antibiofilm activity observations. After the treatment, the pegs were rinsed again and placed into a fresh, AMP-free medium in a biofilm recovery plate. The plate was then sonicated for 30 min to dislodge the biofilm from the pegs into the medium. Serial 10-fold dilutions of each sample, including positive and negative controls, were plated on NB-agar. The plates were incubated for 24 h at 37 °C, and the minimum biofilm eradication concentration (MBEC) was determined based on colony counting.

Proteolytic Stability. Peptides loaded onto MSNs, as described above at pH 10, were used to investigate the proteolytic protection by incubating 0.42 mg/mL temporin B loaded in 1 mg/mL MSNs and 0.45 mg/mL BmKn2 loaded in 1 mg/mL MSN with proteinase K (10 μg/mL) in PBS at pH 7.4. Mixtures were incubated at 37 °C in a thermoblock. After 4, 8, and 16 h, 100 μL samples were taken, mixed with 100 μL of filtered-sterilized H_2O with 0.1% v/v TFA to quench the reaction, centrifuged at 12 000 rpm for 10 min, and characterized using an RP-HPLC C18 column at a wavelength of 220 nm and a linear gradient with a mobile phase composed of eluent A (99.9% v/v H_2O, 0.1% v/v TFA) and eluent B (94.9% v/v acetonitrile, 5% v/v H_2O and 0.1% v/v TFA) at a flow rate of 1 mL/min. This method was adapted from a previous study, which utilized a similar approach to evaluate the peptide stability.[40]

In Vitro Cytotoxicity Assay. Lung fibroblasts (MRC-5) were grown at 37 °C in a controlled atmosphere containing 5% CO_2 according to the supplier instructions. 1×10^4 cells/well were seeded in 96-well plates. The day after seeding, AMP-loaded MSNs were added with a serial dilution of 1:5, with six different concentrations in triplicate, with concentrations ranging from 0.5 mg/mL for the AMPs. After 96 h, the cell viability was measured using CellTiter-Glo (Promega, Madison, WI, USA) with BioTek Synergy H1. Logarithmic dose−response curves were used to calculate the IC_{50} using GraphPad Prism (La Jolla, CA, US). Averages were obtained from triplicate, and the errors are standard deviations.

RESULTS

MSNs were synthesized using a sol−gel method following the procedure detailed in the Materials and Methods section. The mean pore size of the particles was about 2.5 nm, as determined by nitrogen sorption analysis with the BJH method. The specific surface area SBET was 1165 m^2/g, and pore volume 0.6 cm^3/g. The isotherm, shown in Figure 1a, is a type IV (according to the IUPAC classification). Representative electron microscopy images of MSNs are shown in Figure 1b, and the particle size, obtained from scanning electron

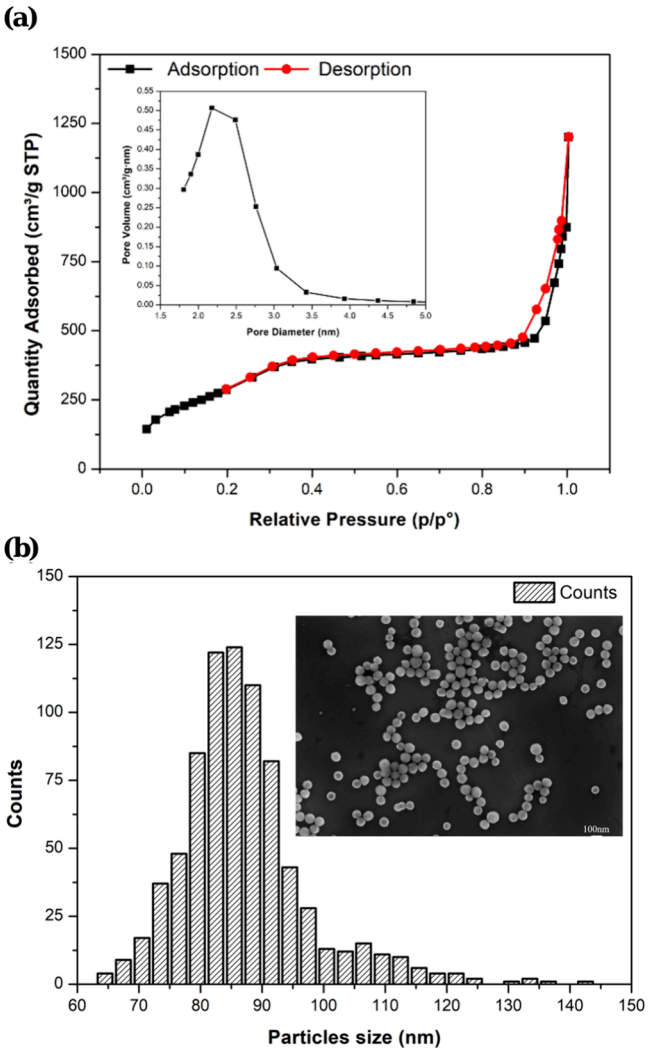

Figure 1. Characterization of MSNs. (a) Nitrogen adsorption−desorption isotherm and pore size distribution of MSNs, confirming the mesoporous structure. (b) Particle size distribution determined by dimensional analysis of SEM images.

https://doi.org/10.1021/acsomega.1c04410
ACS Omega 2025, 10, 60142−60151

microscopy (SEM) images analyzed using ImageJ software, shows a monodisperse distribution centered at 85 nm.

Adsorption of the AMPs temporin B and BmKn2 onto the MSNs was performed in PBS. The optimal peptide loading occurred at pH 10, where the highest adsorption capacity was observed. The loading efficiency for each peptide was quantified using the drug loading capacity (DLS%), calculated as follows:

$$\mathrm{DLC\%} = \frac{\mathrm{drug}_{\mathrm{added}} - \mathrm{drug}_{\mathrm{free}}}{\mathrm{drug}_{\mathrm{added}}} \times 100$$

Here, $\mathrm{drug}_{\mathrm{added}}$ represents the initial amount of the peptide introduced into the MSNs, while $\mathrm{drug}_{\mathrm{free}}$ indicates the amount of peptide remaining in the supernatant (i.e., not loaded within the MSNs).

To evaluate the release behavior of the peptides, the cumulative release (Cr%) over time was calculated using the following formula:

$$\mathrm{Cr\%} = \frac{\mathrm{drug}_{\mathrm{free}}}{\mathrm{drug}_{\mathrm{total}}} \times 100$$

In the above formula, $\mathrm{drug}_{\mathrm{total}}$ refers to the total amount of the peptide loaded into the MSNs, and $\mathrm{drug}_{\mathrm{free}}$ corresponds to the amount released in the solution over time, as determined by the RP-HPLC analysis.

Both the drug loading capacity and cumulative release profiles were found to be pH-dependent, as shown in Table S1 and Figure 2a,b. The adsorption and subsequent release behavior of the AMPs temporin B and BmKn2 varied significantly with pH. At alkaline pH (pH 10), peptide adsorption onto MSNs was enhanced, whereas acidic conditions (pH 5.5) promoted peptide release. Specifically, at pH 10, BmKn2 demonstrated a slightly higher adsorption efficiency than temporin B, achieving maximum adsorption concentrations of 0.45 and 0.42 mg/mL, respectively, in the presence of 1 mg/mL MSNs. Based on the estimated molecular volumes (1680 Å^3 for temporin B and 1700 Å^3 for BmKn2), the total peptide volumes adsorbed per gram of MSNs were calculated to be approximately 0.30 and 0.33 cm^3/g, respectively. These values are well within the measured pore volume of the MSNs (0.6 cm^3/g), supporting the hypothesis that the peptides are predominantly adsorbed within the mesoporous network. Moreover, the approximately 2 nm size of each peptide is smaller than the average MSN pore diameter (2.5 nm), which further supports this conclusion. In terms of the release behavior, both peptides exhibited rapid release under acidic conditions (pH 5.5), with significant release accruing during the 24 h of testing. Temporin B showed a maximum release of 81% of its loading amount, while BmKn2 exhibited 89% release under the same conditions. As the pH increases, the surface of the MSNs becomes more negatively charged, enhancing electrostatic interaction with the cationic peptides. Notably, BmKn2 carries two positive charges, while temporin B carries only one, which likely accounts for the higher adsorption efficiency of BmKn2 (Figure S3). At physiological pH (7.4), the peptide release was minimal (~10%), indicating that MSNs can retain a substantial portion of the loaded peptide under neutral conditions. This suggests that for compartments where the pH is close to neutral, premature peptide release is minimized. Upon arrival at the infection site, where the microenvironment tends to be more

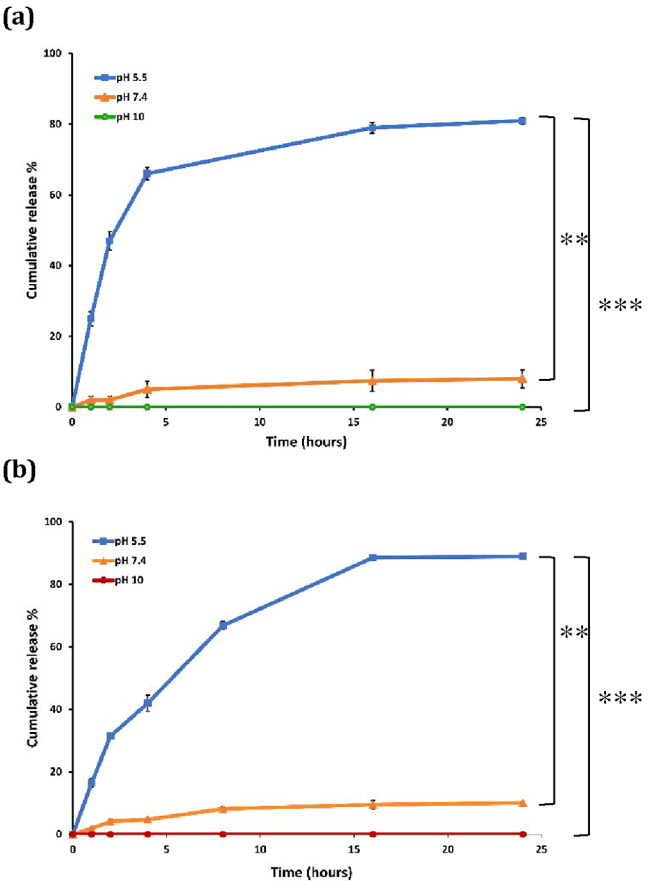

Figure 2. pH-dependent release profiles of the peptide-loaded MSNs. (a) Cumulative release of temporin B from MSNs at pH values of 5.5, 7.4, and 10. (b) Cumulative release of BmKn2 from MSNs at pH values of 5.5, 7.4, and 10. Data are shown as mean ± SEM (n = 3). Statistical differences among pH conditions were analyzed using one-way ANOVA followed by Tukey's multiple comparisons test (α = 0.05). Significant increases in peptide release were observed at acidic pH (5.5) compared with neutral (7.4) and basic (10.0) conditions. p < 0.05 was considered statistically significant. * = p < 0.05; ** = p < 0.01; *** = p < 0.001; ns = not significant. Complete statistical details are provided in Tables S2 and S3.

acidic for *S. aureus*, the MSNs trigger a pH-responsive release. This pH-responsive release behavior enables targeted delivery of AMPs specifically at the pathological area such as infected tissue. As a result, the system is enhanced selectively while reducing off-target toxicity often associated with the passive diffusion-based drug-delivery.

The antibacterial efficacy of peptide-loaded MNSs was evaluated in vitro against *Staphylococcus aureus* ATCC 25923 (Figure 3a–d). MSNs loaded with temporin B were tested at an initial concentration of 133 μg/mL, while BmKn2-loaded MSNs were tested at 50 μg/mL with serial dilutions down to 1 μg/mL. An equivalent concentration of free peptide was used for comparison, based on their respective release profiles. The minimum inhibition concentrations (MICs) of the peptide-loaded MSNs were comparable to those of the free peptides: complete bacterial inhibition was observed at 16 μg/mL for temporin B and 6.25 μg/mL for BmKn2. Importantly, unloaded MSNs showed no antibacterial activity, confirming that the antibacterial activity was due solely to the peptides. The optical density measurement at 600 nm ($\mathrm{OD}_{600\ \mathrm{nm}}$), shown in Figure 3a,b, reflects bacterial growth inhibition and

https://doi.org/10.1021/acsomega.1c04410
ACS Omega 2025, 10, 60142−60151

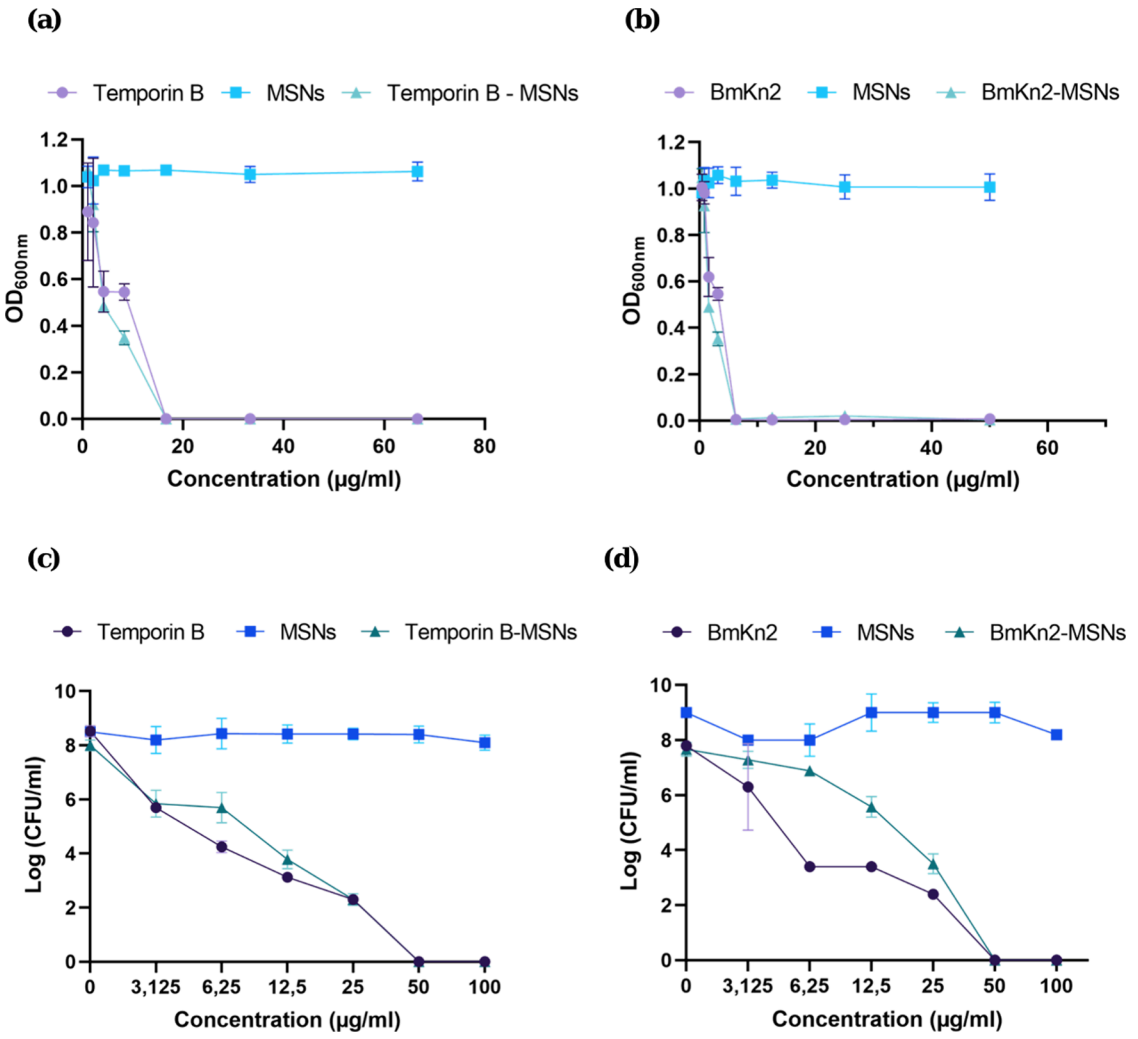

Figure 3. Antimicrobial and antibiofilm activities of free peptides, MSNs, and peptide-loaded MSNs against *Staphylococcus aureus* ATCC 25923. (a) Planktonic bacterial growth following treatment with free temporin B, free MSNs, and temporin B-loaded MSNs. (b) Planktonic bacterial growth following treatment with free BmKn2, free MSNs, and BmKn2-loaded MSNs. (c) Eradication of biofilm by free temporin B, free MSNs, and temporin B-loaded MSNs. (d) Eradication of biofilm by free BmKn2, free MSNs, and BmKn2-loaded MSNs. MSNs were tested at silica concentrations equivalent to those in the respective peptide−MSN formulations. Data are shown as mean ± SEM (n = 3). Statistical comparisons were performed using Welch's ANOVA followed by Dunnett's T3 multiple comparisons test (α = 0.05). $p < 0.05$ was considered statistically significant. *$p < 0.05$; **$p < 0.01$; ns = not significant. Detailed statistical results, including mean differences, 95% confidence intervals, adjusted p-values, and significance levels, are provided in Table S4.

correlates the MIC values observed. To ensure accurate quantification, the background absorbance due to MSNs was accounted for by subtracting the $OD_{600\ nm}$ of the corresponding MSN-only controls (MSN without peptide or bacteria) for each concentration. This correction confirmed that the MSNs themselves did not interfere with or influence the absorbance measurement at 600 nm.

To further evaluate efficacy, we assessed the antibiofilm activity of temporin B-MSNs and BmKn2-MSNs against an *S. aureus* mature biofilm using CBD (Figure 3c,d). The biofilm was treated with both free peptide and peptide-loaded MSNs at serial diluted concentrations. The MBEC for both peptides was determined to be 50 μg/mL, at which no viable colonies were detected after 24 h. As expected, empty MSNs had no antibiofilm activity, confirming that biofilm eradication was due to the antimicrobial properties of the peptides themselves.

In addition to their antibiofilm activity, MSNs also conferred protection to the peptides against enzymatic degradation. To assess this, we investigated the stability of the free peptide and MSN-loaded peptides in the presence of proteinase K, a broad-spectrum protease. Free peptides were incubated with the enzyme for 10, 30, and 60 min, while peptide-loaded MSNs were incubated with the enzyme for extended periods (4, 8, and 16 h) at 37 °C. Chromatographic analysis (Figure 4a−d) revealed that free peptides were rapidly degraded, with significant cleavages occurring as early as 10 min and near complete degradation by 60 min. In contrast, peptides loaded onto the MSNs showed minimal degradation even after 16 h, with degradation corresponding only to the amount released during incubation. This protection is likely due to the steric hindrance provided by the silica matrix, which shields the encapsulated peptides from enzymatic access. The RP-HPLC analysis was performed after using Milli-Q water containing 0.1% trifluoracetic acid showed that acidification triggers peptide release from the MSNs. Importantly, lowered pH also resulted in proteinase K denaturation, further protecting the released peptide from degradation prior to analysis. As shown in Figure 4a,b (temporin B) and Figure 4c,d (BmKn2),

https://doi.org/10.1021/acsomega.1c04410
ACS Omega 2025, 10, 60142−60151

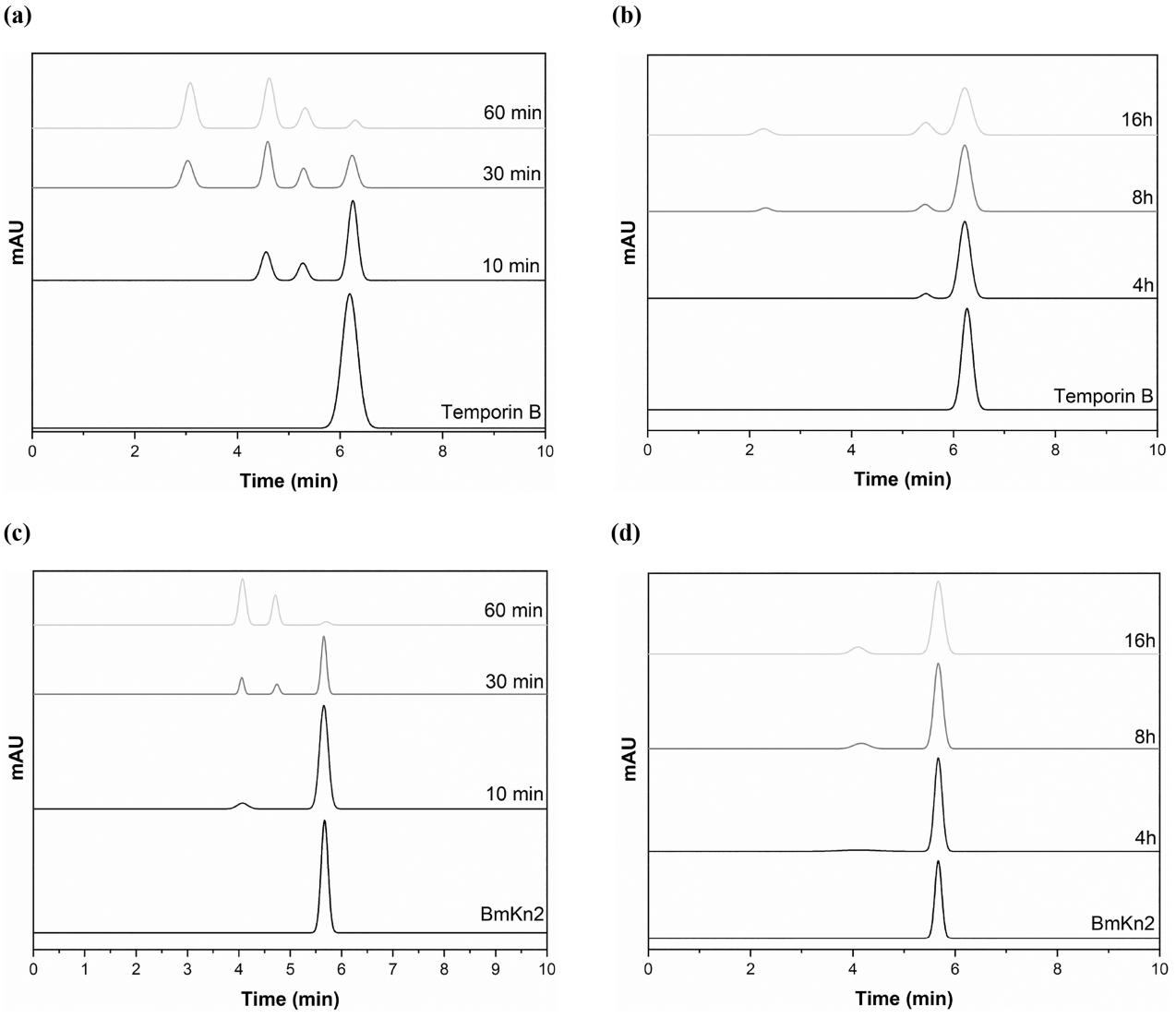

Figure 4. Enzymatic degradation of peptides by proteinase K. (a) Digestion of free temporin B by proteinase K. (b) Digestion of temporin B loaded into MSNs (temporin B-MSNs). (c) Digestion of free BmKn2 by proteinase K. (d) Digestion of BmKn2 loaded into MSNs (BmKn2-MSNs). The assay evaluates the protective effect of MSNs on peptide stability against enzymatic degradation.

peptides released at pH 7.4 retained their integrity with only minor cleavage observed, confirming the protective and controlled release functionality of MSNs.

To evaluate the biocompatibility, we evaluated cytotoxicity using normal lung fibroblast cells (MRC-5). Cells were treated with various concentrations of free peptide and peptide-loaded MSNs. As shown in Figure 5a,b, neither free peptide nor temporin B-loaded MSNs caused significant cytotoxicity, with the cell viability exceeding 90% across all tested concentrations. Notably, BmKn2-MSNs exhibited reduced cytotoxicity compared to the free peptide, particularly at higher concentrations (IC_{50} = 201 μg/mL), suggesting that loading within MSNs mitigates peptide-associated toxicity. A previous work from our group also confirmed the biocompatibility of MSNs alone.[39]

These findings suggest that MSNs not only provide a protective environment for the peptides but also mitigate their potential toxic effects on healthy cells.

DISCUSSION

MSNs were selected as a delivery platform for this study due to their high stability, low cost, and biocompatibility, making them ideal models for biomedical applications.[41] The escalating rates of antimicrobial resistance have underscored the urgent need to develop new therapeutic strategies against drug-resistant pathogens. AMPs, part of the innate immune system, offer a promising alternative to conventional antibiotics due to their broad-spectrum activity and minimal risk of resistance development.[42] However, the direct application of the AMPs in clinical settings is limited due to their inherent low stability and consequently poor bioavailability.[43] Several recent reviews have highlighted the advantages and limitations of various nanocarrier systems for AMP delivery. For example, lipid, polymeric, and metal nanosystems have been compared, with emphasis on issues such as instability, toxicity, and limited control over the release in physiological vs pathological environments.[44] Other studies have focused specifically on biofilm-forming infections, showing that carrier penetration and sustained delivery in acidic microenvironments remain major challenges.[45] To address these limitations, we success-

https://doi.org/10.1021/acsomega.1c04410
ACS Omega 2025, 10, 60142−60151

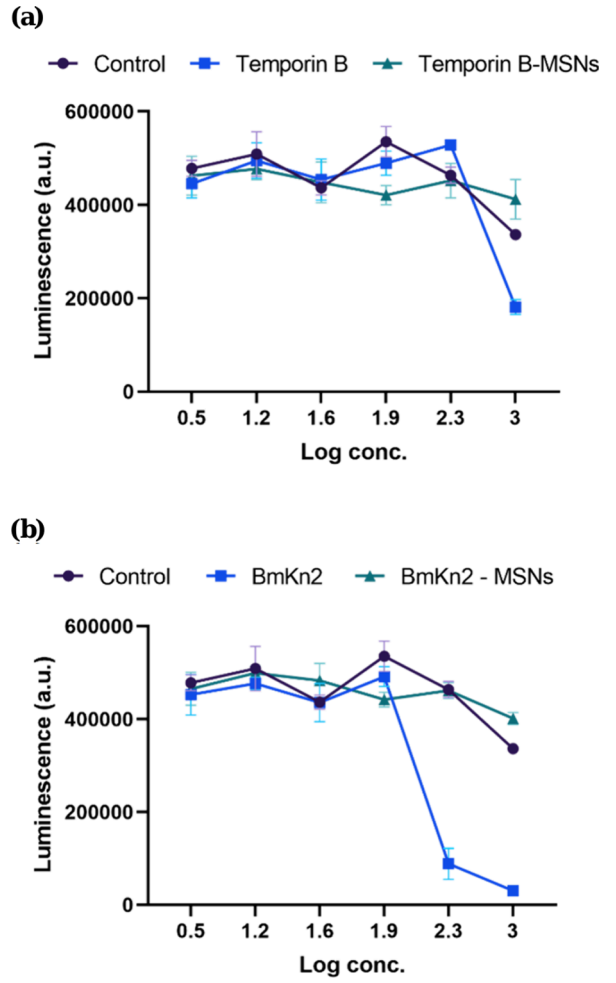

Figure 5. Cytotoxic evaluation of peptide formulations. (a) Cytotoxicity of free temporin B and temporin B-loaded MSNs compared to the untreated control. (b) Cytotoxicity of free BmKn2 and BmKn2-loaded MSNs compared to the untreated control. Data are presented as mean ± SEM (n = 3). Statistical analysis was performed using Welch's ANOVA followed by Dunnett's T3 multiple comparisons test (α = 0.05). No statistically significant differences were observed among the treatment groups (p > 0.05). Full statistical details are provided in Table S5.

fully loaded two AMPs temporin B and BmKn2 into MSNs, achieving peptide loading and controlled release behavior. The pH-responsive nature of the MSNs allows for selective peptide release at infection sites characterized by acidic environments, while minimizing premature release in physiological conditions (pH 7.4). This targeted delivery is crucial in enhancing therapeutic efficacy and reducing systemic toxicity, as confirmed by the low release observed at pH 7.4 and the significant release at pH 5.5 as detailed in the release profiles (Figure 2). Our in vitro studies demonstrated that the loaded AMPs retained their antibacterial and antibiofilm activities. Specifically, the MIC values for both peptide-loaded MSNs were similar to those of the free peptides, showing complete inhibition of *Staphylococcus aureus* ATCC25923 at 16 μg/mL for Temporin B and 6.25 μg/mL for BmKn2 (Figure 3a,b). This indicates that the activity of the peptides is preserved after loading and release, underscoring the protective roles of MSNs against potential degradation in biological environments. Additionally, the antibiofilm assays using CBD for both temporin B and BmKn2, when loaded into MSNs, effectively eradicated a mature biofilm at a concentration of 50 μg/mL, as evidenced by the absence of viable bacterial colonies after treatment (Figure 3c,d). The antibiofilm activity is particularly relevant for tracking persistent infections associated with medical devices where biofilm formation contributes to increased resistance and recurrence. One of the significant challenges in AMP development is their susceptibility to proteolytic degradation.[46] Our study demonstrated that the MSNs provide a protective environment for the peptides, preventing rapid enzymatic breakdown. Free peptides were almost entirely degraded by proteinase K within 60 min, while those loaded into MSNs were protected from proteolytic degradation even after 16 h of incubation (Figure 4). This suggests that the MSNs effectively shield the peptides from proteolytic degradation, likely due to steric hindrance where the large enzyme molecules are unable to access the peptides loaded within the nanopores.[47] The pH-triggered release mechanism of MSNs further enhances their protective capability. When the peptide-loaded MSNs were exposed to acidic conditions, the release of the peptides was initiated, while the activity of proteinase K was simultaneously inhibited by the drop in pH. This dual functionality ensures that the peptides are released in an active form only when they reach the targeted infection site, minimizing their therapeutic potential.

The mechanism of action of temporin B and BmKn2 (Scheme 1) seems to be dependent on its interaction with the microbial membranes, similar to what has been demonstrated for many other AMPs. The first step in this interaction is the electrostatic attraction between the cationic peptide and the negatively charged components of the bacterial cell wall. After that, the peptide reaches the inner membrane, perturbing its permeability and causing rapid cell death.[22] AMP delivery through nanocarriers, as the MSNs used in this study, has the potential to be employed in a wide range of applications.[30] Pathological conditions that could particularly benefit from the use of such nanosystems are those that occur at mucosal/skin surfaces and require multiple (daily) and long-term drug administrations for the prevention/treatment of microbial infections. These conditions might include wound infections in burn or diabetic patients.[48] The low tendency to induce bacterial resistance of the delivered AMPs, and the strong antibacterial properties, together with the continuous release kinetics, are all properties that could likely contribute to the long-lasting control of microbial infections in the above-mentioned conditions, meanwhile reducing the number of drug administrations and increasing the compliance of the patient.[49] In our study, *S. aureus* was used as a model Gram-positive bacterium. Temporin B and BmKn2 have also previously shown activity against a broad range of nosocomial Gram-positive and, to a lesser extent, Gram-negative strains.[37,38,50] Thus, the nanocarrier described herein may represent a versatile tool to allow long-term control of microbial infections sustained by different clinically relevant bacterial species.

CONCLUSIONS

The development of AMPs as novel therapeutic agents holds great promise in addressing the growing challenge of drug-resistant bacterial infections. However, the clinical application of AMPs has been limited by their low stability, rapid degradation, and low bioavailability. In this work, we successfully loaded two model alfahelical AMPs, temporin B

https://doi.org/10.1021/acsomega.1c04410
ACS Omega 2025, 10, 60142−60151

Scheme 1. Possible Delivery Mechanism of Temporin B and BmKn2

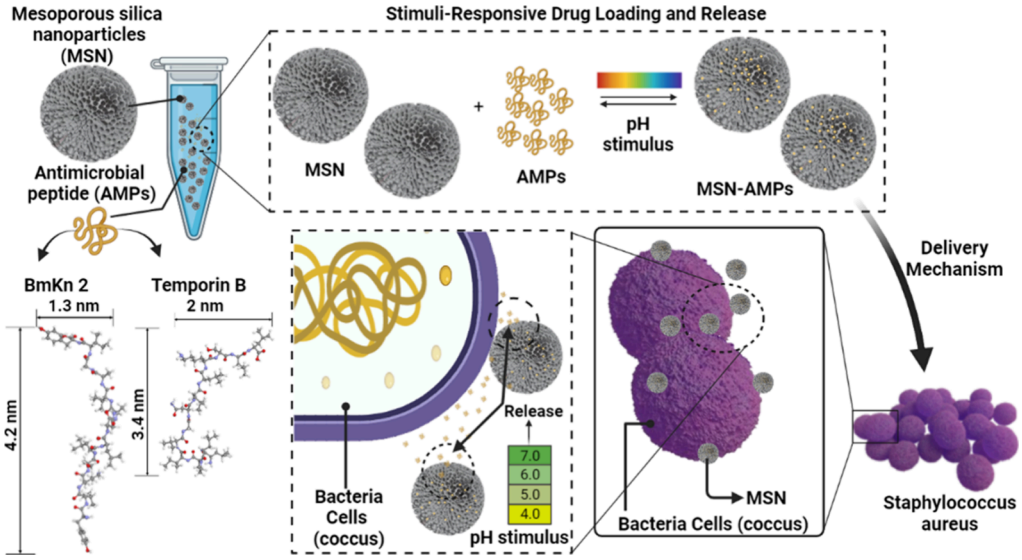

and BmKn2, into MSNs. The results demonstrated that this nanosystem provides multiple advantages: it enhances peptide stability by protecting against enzymatic degradation, enables pH-responsive release, and retains the bactericidal and antibiofilm activity against *Staphylococcus aureus*, a clinically relevant pathogen. This study targets both planktonic bacteria and biofilm-associated infections, the latter being notably more resistant to standard treatments. The protective effect of MSNs against proteolytic degradation is a critical factor for in vivo applications, where AMPs are exposed to various proteolytic enzymes, which can limit their therapeutic potential. Additionally, pH-responsive release is a key feature for achieving high therapeutic concentrations at the site of infection while minimizing side effects. While the in vitro findings of our study are encouraging, further in *vivo* or ex vivo studies are essential to validate the therapeutic potential of the nanosystem. Future research should focus on evaluating the biodistribution, pharmacokinetics, and pharmacodynamics of MSNs-loaded AMPs in an animal model of infection.

Additionally, exploring the efficacy of this delivery system against a broader range of pathogens, including Gram-negative bacteria and multiresistant strains, will provide valuable insights into its versatility and clinical applicability. Moreover, the adaptability of the MSNs to load various AMPs or other therapeutic agents suggests that this platform could be tailored to combination therapies. By codelivering AMPs with conventional antibiotics or other antimicrobial agents, it may be possible to enhance the overall antibacterial efficacy and reduce the likelihood of resistance development.

The successful translation of such nanosystems into clinical practices could mark a significant advancement in the fight against antimicrobial resistance, offering new strategies to enhance the effectiveness of peptide-based therapeutics and improve patient outcomes.

■ ASSOCIATED CONTENT

Supporting Information

The Supporting Information is available free of charge at https://pubs.acs.org/doi/10.1021/acsomega.1c04410.

LC/MS analysis of molecular mass temporin B and BmKn2 (confirmation of the molecular mass using LC-MS) (Figure S1); calibration curves of temporin B and BmKn2 analyzed with RP-HPLC (establishment of the calibration curves for temporin B and BmKn2 using HPLC) (Figure S2); ζ-potential analysis of peptides and MSNs (Figure S3); drug loading capacity (DLC%) and cumulative release (Cr%) (Table S1); statistical analysis of temporin B release from MSNs (Table S2); statistical analysis of BmKn2 release from MSNs (Table S3); statistical comparisons of antibacterial and antibiofilm measurements (Table S4); and statistical comparisons of cytotoxicity measurements (Table S5) (PDF)

■ AUTHOR INFORMATION

Corresponding Author

Mirena Sakaj − *Department of Molecular Sciences and Nanosystems, Ca' Foscari University of Venice, 30172 Mestre, Italy;* Present Address: Stippeneng 4, 6708WE Wageningen, The Netherlands; orcid.org/0000-0001-7144-2154; Email: mirena.sakaj@wur.nl

Authors

Vincenzo Lombardi − *Department of Molecular Sciences and Nanosystems, Ca' Foscari University of Venice, 30172 Mestre, Italy*

Isabella Caligiuri − *Pathology Unit Department of Molecular Biology and Translational Research, Centro di Riferimento Oncologico di Aviano (CRO) IRCCS, 33081 Aviano, Italy*

Andrea Castellin − *Brenta Srl, 36075 Vicenza, Italy*

Pietro Riello − *Department of Molecular Sciences and Nanosystems, Ca' Foscari University of Venice, 30172 Mestre, Italy; European Centre for Living Technology (ECLT), 30123 Venice, Italy;* orcid.org/0000-0002-6087-3802

Complete contact information is available at: https://pubs.acs.org/10.1021/acsomega.1c04410

Author Contributions

The manuscript was written through contributions of all authors. All authors have given approval to the last version of the manuscript.

Notes

The authors declare no competing financial interest.

https://doi.org/10.1021/acsomega.1c04410
ACS Omega 2025, 10, 60142−60151

■ ACKNOWLEDGMENTS

The authors are grateful to all of the group members for the helpful discussions and technical assistance. The authors also gratefully acknowledge Prof. Alessandro Angelini for his valuable support and guidance that helped shape the initial direction of this work. The financial contribution from Brenta S.r.l. is gratefully acknowledged. TOC was created with Biorender.

■ REFERENCES

(1) Blaskovich, M. A. T. Antibiotics Special Issue: Challenges and Opportunities in Antibiotic Discovery and Development. *ACS Infect. Dis.* **2020**, *6* (6), 1286−1288.
(2) McFee, R. B. Nosocomial or Hospital-Acquired Infections: An Overview. *Disease-a-Month* **2009**, *55* (7), 422−438.
(3) Hofer, U. The Cost of Antimicrobial Resistance. *Nat. Rev. Microbiol* **2019**, *17* (1), 3−3.
(4) Bouchiat, C.; Curtis, S.; Spiliopoulou, I.; Bes, M.; Cocuzza, C.; Codita, I.; Dupieux, C.; Giormezis, N.; Kearns, A.; Laurent, F.; Molinos, S.; Musumeci, R.; Prat, C.; Saadatian-Elahi, M.; Tacconelli, E.; Tristan, A.; Schulte, B.; Vandenesch, F. MRSA Infections among Patients in the Emergency Department: A European Multicentre Study. *J. Antimicrob. Chemother.* **2017**, *72* (2), 372−375.
(5) Habib, G.; Lancellotti, P.; Antunes, M. J.; Bongiorni, M. G.; Casalta, J.-P.; Del Zotti, F.; Dulgheru, R.; El Khoury, G.; Erba, P. A.; Iung, B.; Miro, J. M.; Mulder, B. J.; Plonska-Gosciniak, E.; Price, S.; Roos-Hesselink, J.; Snygg-Martin, U.; Thuny, F.; Tornos Mas, P.; Vilacosta, I.; Zamorano, J. L. 2015 ESC Guidelines for the Management of Infective Endocarditis. *Eur. Heart J.* **2015**, *36* (44), 3075−3128.
(6) Kapadia, B. H.; Berg, R. A.; Daley, J. A.; Fritz, J.; Bhave, A.; Mont, M. A. Periprosthetic Joint Infection. *Lancet* **2016**, *387* (10016), 386−394.
(7) Costerton, J. W.; Stewart, P. S.; Greenberg, E. P. Bacterial Biofilms: A Common Cause of Persistent Infections. *Science (1979)* **1999**, *284* (5418), 1318−1322.
(8) de Jong, N. W. M.; van Kessel, K. P. M.; van Strijp, J. A. G. Immune Evasion by Staphylococcus Aureus. *Microbiol. Spectr.* **2019**, *7* (2). .
(9) Banerjee, D.; Shivapriya, P. M.; Gautam, P. K.; Misra, K.; Sahoo, A. K.; Samanta, S. K. A Review on Basic Biology of Bacterial Biofilm Infections and Their Treatments by Nanotechnology-Based Approaches. *Proceedings of the National Academy of Sciences, India Section B: Biological Sciences* **2020**, *90* (2), 243−259.
(10) Römling, U.; Kjelleberg, S.; Normark, S.; Nyman, L.; Uhlin, B. E.; Åkerlund, B. Microbial Biofilm Formation: A Need to Act. *J. Intern Med.* **2014**, *276* (2), 98−110.
(11) Høiby, N.; Bjarnsholt, T.; Givskov, M.; Molin, S.; Ciofu, O. Antibiotic Resistance of Bacterial Biofilms. *Int. J. Antimicrob. Agents* **2010**, *35* (4), 322−332.
(12) Baudoux, P.; Bles, N.; Lemaire, S.; Mingeot-Leclercq, M.-P.; Tulkens, P. M.; Van Bambeke, F. Combined Effect of PH and Concentration on the Activities of Gentamicin and Oxacillin against Staphylococcus Aureus in Pharmacodynamic Models of Extracellular and Intracellular Infections. *J. Antimicrob. Chemother.* **2006**, *59* (2), 246−253.
(13) Davies, D. G.; Marques, C. N. H. A Fatty Acid Messenger Is Responsible for Inducing Dispersion in Microbial Biofilms. *J. Bacteriol.* **2009**, *191* (5), 1393−1403.
(14) Zhou, C.; Fey, P. D. The Acid Response Network of Staphylococcus Aureus. *Curr. Opin Microbiol* **2020**, *55*, 67−73.
(15) Subbarayudu, S.; Snega priya, P.; Rajagopal, R.; Alfarhan, A.; Guru, A.; Arockiaraj, J. Impact of Acidic and Alkaline Conditions on Staphylococcus Aureus and Acinetobacter Baumannii Interactions and Their Biofilms. *Arch. Microbiol.* **2024**, *206* (11), 426.
(16) Bæk, K. T.; Gründling, A.; Mogensen, R. G.; Thøgersen, L.; Petersen, A.; Paulander, W.; Frees, D. β-Lactam Resistance in Methicillin-Resistant Staphylococcus Aureus USA300 Is Increased by Inactivation of the ClpXP Protease. *Antimicrob. Agents Chemother.* **2014**, *58* (8), 4593−4603.
(17) Choo, E. J.; Chambers, H. F. Treatment of Methicillin-Resistant Staphylococcus Aureus Bacteremia. *Infect Chemother* **2016**, *48* (4), No. 267.
(18) Cong, Y.; Yang, S.; Rao, X. Vancomycin Resistant Staphylococcus Aureus Infections: A Review of Case Updating and Clinical Features. *J. Adv. Res.* **2020**, *21*, 169−176.
(19) Hancock, R. E. W.; Sahl, H.-G. Antimicrobial and Host-Defense Peptides as New Anti-Infective Therapeutic Strategies. *Nat. Biotechnol.* **2006**, *24* (12), 1551−1557.
(20) Koehbach, J.; Craik, D. J. The Vast Structural Diversity of Antimicrobial Peptides. *Trends Pharmacol. Sci.* **2019**, *40* (7), 517−528.
(21) Feng, Q.; Huang, Y.; Chen, M.; Li, G.; Chen, Y. Functional Synergy of α-Helical Antimicrobial Peptides and Traditional Antibiotics against Gram-Negative and Gram-Positive Bacteria in Vitro and in Vivo. *European Journal of Clinical Microbiology & Infectious Diseases* **2015**, *34* (1), 197−204.
(22) Raheem, N.; Straus, S. K. Mechanisms of Action for Antimicrobial Peptides With Antibacterial and Antibiofilm Functions. *Front Microbiol* **2019**, *10*, 10.
(23) Zhang, Q.-Y.; Yan, Z.-B.; Meng, Y.-M.; Hong, X.-Y.; Shao, G.; Ma, J.-J.; Cheng, X.-R.; Liu, J.; Kang, J.; Fu, C.-Y. Antimicrobial Peptides: Mechanism of Action, Activity and Clinical Potential. *Mil Med. Res.* **2021**, *8* (1), 48.
(24) Gaspar, D.; Veiga, A. S.; Castanho, M. A. R. B. From Antimicrobial to Anticancer Peptides. *A Review. Front Microbiol* **2013**, *4*, No. 4.
(25) Pasupuleti, M.; Schmidtchen, A.; Malmsten, M. Antimicrobial Peptides: Key Components of the Innate Immune System. *Crit Rev. Biotechnol* **2012**, *32* (2), 143−171.
(26) Yu, G.; Baeder, D. Y.; Regoes, R. R.; Rolff, J. Combination Effects of Antimicrobial Peptides. *Antimicrob. Agents Chemother.* **2016**, *60* (3), 1717−1724.
(27) Drayton, M.; Kizhakkedathu, J. N.; Straus, S. K. Towards Robust Delivery of Antimicrobial Peptides to Combat Bacterial Resistance. *Molecules* **2020**, *25* (13), No. 3048.
(28) Pal, I.; Bhattacharyya, D.; Kar, R. K.; Zarena, D.; Bhunia, A.; Atreya, H. S. A Peptide-Nanoparticle System with Improved Efficacy against Multidrug Resistant Bacteria. *Sci. Rep* **2019**, *9* (1), 4485.
(29) Teixeira, M. C.; Carbone, C.; Sousa, M. C.; Espina, M.; Garcia, M. L.; Sanchez-Lopez, E.; Souto, E. B. Nanomedicines for the Delivery of Antimicrobial Peptides (AMPs). *Nanomaterials* **2020**, *10* (3), No. 560.
(30) Malmsten, M. Inorganic Nanomaterials as Delivery Systems for Proteins, Peptides, DNA, and SiRNA. *Curr. Opin. Colloid Interface Sci.* **2013**, *18* (5), 468−480.
(31) Biswaro, L. S.; da Costa Sousa, M. G.; Rezende, T. M. B.; Dias, S. C.; Franco, O. L. Antimicrobial Peptides and Nanotechnology, Recent Advances and Challenges. *Front Microbiol* **2018**, *9*, 9.
(32) Zhou, Y.; Quan, G.; Wu, Q.; Zhang, X.; Niu, B.; Wu, B.; Huang, Y.; Pan, X.; Wu, C. Mesoporous Silica Nanoparticles for Drug and Gene Delivery. *Acta Pharm. Sin B* **2018**, *8* (2), 165−177.
(33) Argyo, C.; Weiss, V.; Bräuchle, C.; Bein, T. Multifunctional Mesoporous Silica Nanoparticles as a Universal Platform for Drug Delivery. *Chem. Mater.* **2014**, *26* (1), 435−451.
(34) Selvarajan, V.; Obuobi, S.; Ee, P. L. R. Silica Nanoparticles—A Versatile Tool for the Treatment of Bacterial Infections. *Front Chem.* **2020**, *8*, 8.
(35) Yang, K. N.; Zhang, C. Q.; Wang, W.; Wang, P. C.; Zhou, J. P.; Liang, X. J. PH-Responsive Mesoporous Silica Nanoparticles Employed in Controlled Drug Delivery Systems for Cancer Treatment. *Cancer Biol. Med.* **2014**, *11* (1), 34−43.
(36) Namdar, N.; Nayeri Fasaei, B.; Shariati, P.; Joghataei, S. M.; Arpanaei, A. Mesoporous Silica Nanoparticles Co-Loaded with Lysozyme and Vancomycin for Synergistic Antimicrobial Action. *Sci. Rep* **2024**, *14* (1), 29242.

https://doi.org/10.1021/acsomega.1c04410
ACS Omega 2025, 10, 60142−60151

(37) Simmaco, M.; Mignogna, G.; Canofeni, S.; Miele, R.; Mangoni, M. L.; Barra, D. Temporins, Antimicrobial Peptides from the European Red Frog Rana Temporaria. *Eur. J. Biochem.* **1996**, *242* (3), 788−792.
(38) Cao, L.; Dai, C.; Li, Z.; Fan, Z.; Song, Y.; Wu, Y.; Cao, Z.; Li, W. Antibacterial Activity and Mechanism of a Scorpion Venom Peptide Derivative In Vitro and In Vivo. *PLoS One* **2012**, *7* (7), No. e40135.
(39) Sponchia, G.; Marin, R.; Freris, I.; Marchiori, M.; Moretti, E.; Storaro, L.; Canton, P.; Lausi, A.; Benedetti, A.; Riello, P. Mesoporous Silica Nanoparticles with Tunable Pore Size for Tailored Gold Nanoparticles. *J. Nanopart. Res.* **2014**, *16* (2), 2245.
(40) Angelini, A.; Morales-Sanfrutos, J.; Diderich, P.; Chen, S.; Heinis, C. Bicyclization and Tethering to Albumin Yields Long-Acting Peptide Antagonists. *J. Med. Chem.* **2012**, *55* (22), 10187−10197.
(41) Ahmed, H.; Gomte, S. S.; Prathyusha, E.; A, P.; Agrawal, M.; Alexander, A. Biomedical Applications of Mesoporous Silica Nanoparticles as a Drug Delivery Carrier. *J. Drug Deliv Sci. Technol.* **2022**, *76*, No. 103729.
(42) Magana, M.; Pushpanathan, M.; Santos, A. L.; Leanse, L.; Fernandez, M.; Ioannidis, A.; Giulianotti, M. A.; Apidianakis, Y.; Bradfute, S.; Ferguson, A. L.; Cherkasov, A.; Seleem, M. N.; Pinilla, C.; de la Fuente-Nunez, C.; Lazaridis, T.; Dai, T.; Houghten, R. A.; Hancock, R. E. W.; Tegos, G. P. The Value of Antimicrobial Peptides in the Age of Resistance. *Lancet Infect Dis* **2020**, *20* (9), e216−e230.
(43) Lai, Z.; Yuan, X.; Chen, H.; Zhu, Y.; Dong, N.; Shan, A. Strategies Employed in the Design of Antimicrobial Peptides with Enhanced Proteolytic Stability. *Biotechnol Adv.* **2022**, *59*, No. 107962.
(44) de Oliveira, K. B. S.; Leite, M. L.; Melo, N. T. M.; Lima, L. F.; Barbosa, T. C. Q.; Carmo, N. L.; Melo, D. A. B.; Paes, H. C.; Franco, O. L. Antimicrobial Peptide Delivery Systems as Promising Tools Against Resistant Bacterial Infections. *Antibiotics* **2024**, *13* (11), No. 1042.
(45) Campos, J. V.; Pontes, J. T. C.; Canales, C. S. C.; Roque-Borda, C. A.; Pavan, F. R. Advancing Nanotechnology: Targeting Biofilm-Forming Bacteria with Antimicrobial Peptides. *BME Front.* **2025**, *6*, No. 0104.
(46) Lyu, Y.; Yang, Y.; Li, P.; Zhou, C.; Zhang, L.; Bi, C.; Shan, A. The Effects of Antimicrobial Peptide-Chitosan Nanoparticles on Alleviating Ulcerative Colitis in Citrobacter Rodentium Infected Mice. *Food Biosci* **2025**, *68*, No. 106575.
(47) Xu, C.; Lei, C.; Yu, C. Mesoporous Silica Nanoparticles for Protein Protection and Delivery. *Front Chem.* **2019**, *7*, 7.
(48) Haidari, H.; Melguizo-Rodríguez, L.; Cowin, A. J.; Kopecki, Z. Therapeutic Potential of Antimicrobial Peptides for Treatment of Wound Infection. *American Journal of Physiology-Cell Physiology* **2023**, *324* (1), C29−C38.
(49) Elbediwi, M.; Rolff, J. Metabolic Pathways and Antimicrobial Peptide Resistance in Bacteria. *J. Antimicrob. Chemother.* **2024**, *79* (7), 1473−1483.
(50) Capparelli, R.; Romanelli, A.; Iannaccone, M.; Nocerino, N.; Ripa, R.; Pensato, S.; Pedone, C.; Iannelli, D. Synergistic Antibacterial and Anti-Inflammatory Activity of Temporin A and Modified Temporin B In Vivo. *PLoS One* **2009**, *4* (9), No. e7191.

https://doi.org/10.1021/acsomega.1c04410
ACS Omega 2025, 10, 60142−60151